THE JOURNAL OF PHYSICAL CHEMISTRY B

Article

pubs.acs.org/JPCB

Large Spectral Change due to Amide Modes of a β-Sheet upon the Formation of an Early Photointermediate of Middle Rhodopsin

Yuji Furutani,*[,†,‡] Takashi Okitsu,[§] Louisa Reissig,[∥] Misao Mizuno,[⊥] Michio Homma,[∥] Akimori Wada,[§] Yasuhisa Mizutani,[⊥] and Yuki Sudo*[,‡,∥]

[†]Department of Life and Coordination-Complex Molecular Science, Institute for Molecular Science, 38 Nishigo-Naka, Myodaiji, Okazaki 444-8585, Japan

[‡]PRESTO, Japan Science and Technology Agency (JST), 4-1-8 Honcho Kawaguchi, Saitama, 332-0012, Japan

[§]Graduate School of Organic Chemistry for Life Science, Kobe Pharmaceutical University, Higashinada-ku, Kobe 658-8558, Japan

[∥]Division of Biological Science, Graduate School of Science, Nagoya University, Nagoya, 464-8602, Japan

[⊥]Department of Chemistry, Graduate School of Science, Osaka University, 1-1 Machikaneyama, Toyonaka, Osaka 560-0043, Japan

Supporting Information

ABSTRACT: Rhodopsin contains retinal as the chromophore within seven transmembrane helices. Recently, we found a unique rhodopsin (middle rhodopsin, MR), which is evolutionarily located between the well-studied bacteriorhodopsin and sensory rhodopsin II, and which accommodates three retinal isomers in its ground state (the all-*trans*, the 13-*cis*, and, uniquely, the 11-*cis* isomers). In this study, we investigated structural changes of both the protein moiety and the retinal chromophore during photocycles of MR by time-resolved Fourier-transform infrared spectroscopy. Three photointermediates with decay time constants of 95 μs, 0.9 ms, and >∼10 ms were identified by the global exponential fitting analysis. The first and third intermediates were attributed to the all-*trans* photocycle, in accordance with recently published results, whereas the second intermediate was likely one that was spectroscopically silent in the visible region and that was formed between the first and third states or resulted from the activation of the 13-*cis* isomer. By comparing light-induced difference spectra with various isotope labels in either the retinal or the protein moiety, we concluded that a β-sheet structure in the hydrophilic part was significantly altered during the all-*trans* photocycle of MR, which may involve an active state of the protein. This feature is characteristic of MR among microbial (type-1) rhodopsins.

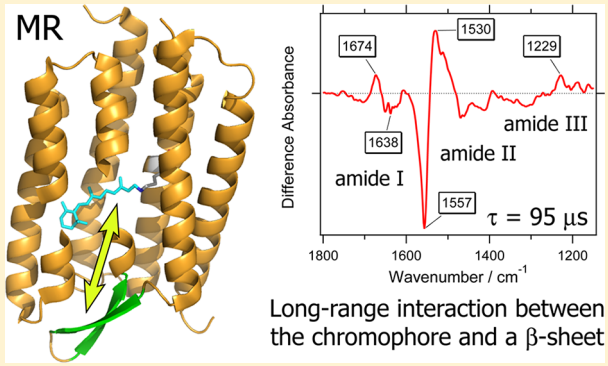

INTRODUCTION

Photoactive proteins are widespread in organisms and function as photoreceptors with their cognate chromophores.[1] Rhodopsins contain vitamin A aldehyde (retinal) as their chromophore within seven transmembrane α-helices and exhibit various colors (with the absorption maximum located between 485 and 580 nm), which correspond to their most probable transition from the electronic ground state to the excited state.[1] On the basis of their origin, they are classified into two groups: microbial (type-1) and animal (type-2) rhodopsins. To a great extent, the functions of type-1 rhodopsins can be divided into light-driven ion transporters and signaling light-sensors, whereas many type-2 rhodopsins found thus far are coupled to a trimeric G-protein and catalyze the GDP−GTP exchange reaction.[1,2]

The biological functions of these rhodopsins are triggered by photoisomerization of the retinal chromophore. Many type-1 rhodopsins contain all-*trans* retinal in the original state, and the retinal chromophore is photoisomerized to a 13-*cis* configuration.[2] In contrast, many type-2 rhodopsins contain 11-*cis* retinal in the original state, and the retinal is photoisomerized to an all-*trans* configuration.[3] Recently, we found a new type-1 rhodopsin molecule from *Haloquadratum walsbyi* (named middle rhodopsin, MR), which was identified as a transition molecule in the evolution from a light-driven proton-pumping rhodopsin [as is bacteriorhodopsin (BR)] to a photosensor for negative phototaxis [sensory rhodopsin II (SRII)].[4] This discovery was based on the facts that the absorption maximum of MR is located at 485 nm in *n*-dodecyl-β-D-maltoside (DDM) micelles, which is more similar to that of SRII (∼500 nm) than to that of BR (∼570 nm), and that the turnover rate of the photocycle of MR is approximately several 10 ms, which, in turn, is more similar to that of BR (∼10 ms) than to that of SRII (∼1 s).[4] Thus, MR exhibits molecular properties that are characteristic of both BR and SRII. On the basis of these results, combined with other findings, we hypothesized that, at

Received: September 4, 2012
Revised: January 19, 2013
Published: March 11, 2013

dx.doi.org/10.1021/jp308765t | J. Phys. Chem. B 2013, 117, 3449−3458

the beginning of the molecular evolution from the ancestor of BR to SRII, color tuning and the insertion of a Thr residue (BR: Ala215, SRII: Thr204), which are critical for the photosensory function, might have occurred.[4]

However, interestingly, a sample of MR contains a significant amount of the 11-*cis* retinal isomer under the dark conditions, and the amount of this retinal isomer greatly increases after light adaptation.[4] Notably, this result represents the first finding of a type-1 rhodopsin that binds 11-*cis* retinal—a feature commonly observed only among type-2 rhodopsins.[3] To induce such a change in the isomeric composition, a large structural rearrangement around the retinal chromophore must occur in MR relative to that required in BR or SRII, because, in the case of 11-*cis* retinal, a double bond (C_{11}=C_{12}) is altered, resulting in a change in the orientation of a methyl group at the C_{13} position, which can be expected to induce a comparably large volume change (i.e., a structural rearrangement). Recently, we identified the absolute absorption spectra of all of the MR isomers by a combination of high-performance liquid chromatography (HPLC) and UV−vis spectroscopy under various light conditions.[5] As a result, the absorption maxima of MR with all-*trans*, 13-*cis*, or 11-*cis* retinal were determined to be located at 485, 479, or 495 nm, respectively.[5] In addition, on the basis of data obtained via time-resolved laser spectroscopy using lasers of various wavelengths, we proposed that the individual photocycles of MR are as follows: MR(*trans*) → MR_K: lifetime = 93 μs → MR_M: lifetime = 12 ms → MR; MR(13-*cis*) → $MR_{O\text{-}like}$: lifetime = 5.1 ms → MR; and MR(11-*cis*) → $MR_{K\text{-}like}$: lifetime = 8.2 μs → MR.[5]

The all-*trans* isomer is expected to form its active form in a light-dependent manner, consistent with the behavior of numerous other type-1 rhodopsins.[1,2] Therefore, herein, we aimed to investigate the light-induced structural changes of the all-*trans* isomer of MR by time-resolved Fourier-transform infrared (TR-FTIR) spectroscopy using samples labeled with stable isotopes. We used a 532 nm laser pulse to excite the sample and to favorably activate the red-shifted isomers that bind to an all-*trans* or 11-*cis* retinal chromophore.[5] In the case of our experimental setup, the fast (8.2 μs) photochemical reaction of the 11-*cis* isomer was not expected to be detected because of insufficient time resolution (12.5 μs). In addition, the intensity of the signal from the 11-*cis* isomer was expected to be diminished because of its low concentration in phosphatidylglycerol (PG) liposomes (9.6%). Thus, herein, we primarily observed spectral changes upon photoisomerization of the all-*trans* isomer. From TR-FTIR studies, the spectral change not only from the amide I and II modes but also from the amide III mode, which typically gives a considerably weaker signal than the amide I and II modes, was observed upon the formation of the intermediate with a decay time constant of 95 μs. In particular, the intensities of the amide II bands were significantly greater than that of an ethylenic C=C stretching mode of the retinal chromophore, which is usually considered as a standard marker band of retinal-containing proteins; this result suggests that a large conformation change occurred in the peptide backbone. On the basis of our observations, we concluded that photoisomerization of all-*trans* retinal in MR induced a large perturbation of a β-sheet structure in the hydrophilic part of MR, which is presumably a unique conformational change not observed in either BR or SRII.

MATERIALS AND METHODS

Sample Preparation. The MR expression plasmid was constructed as previously described.[4] Cells were grown in LB medium supplemented with ampicillin (final concentration: 50 μg/mL). *Escherichia coli* BL21 (DE3) cells harboring the plasmid were grown to an OD660 of 0.3−0.5 in a 30 °C incubator, followed by addition of 0.5 mM isopropyl 1-thio-β-D-galactopyranoside. Retinal analogues (^{13}C at the C_{12} or C_{13} position or deuteration at C_{14}−H or C_{15}−H) were synthesized by standard methods,[6] and each analogue (0.2 mg) was added to the *E. coli* culture (1 L), whereas unlabeled authentic all-*trans* retinal from Sigma-Aldrich was used for the unlabeled samples. For preparation of uniformly ^{13}C-labeled or Tyr (phenol-4-^{13}C)-labeled proteins, transformed cells were initially grown at 30 °C in 1 mL of LB medium and were directly inoculated into 200 mL of isotope-labeled standard minimal M9 medium, i.e., medium that contained 1.0 g/L ^{13}C-D-glucose (Isotec, Miamisburg, OH) or 50 mg/L L-tyrosine (phenol-4-^{13}C, 95−99%) (Cambridge Isotope Laboratories, Andover, MA), followed by inoculation into 10 or 2 L of the labeled mediums, respectively.[7,8]

Cells were harvested 10 h postinduction at 18 °C by centrifugation at 4 °C, were resuspended in buffer I [50 mM 2-(*N*-morpholino)ethanesulfonic acid (MES), 1 M NaCl, pH 6.5], and were disrupted by sonication or a French press. Cell debris was removed by low-speed centrifugation (5000 × *g* for 10 min at 4 °C). Preparation of crude membranes and purification of MR proteins were performed essentially by the same method as that described previously.[4,5,9] Crude membranes were collected by centrifugation (100 000 × *g* for 30 min at 4 °C) and washed with buffer I supplemented with 5 mM imidazole. For solubilization of membranes, 2.5% (w/v) DDM was added, and the suspension was incubated for 30 min at 4 °C. The solubilized membranes were isolated by high-speed centrifugation (100 000 × *g* for 30 min at 4 °C), and the supernatant was applied to a nickel-affinity column (HisTrap, GE Healthcare) at 4 °C in the dark. Thereafter, the column was extensively washed with buffer II (50 mM MES, 1 M NaCl, 20 mM imidazole, 0.05% DDM, pH 6.5) to remove nonspecifically bound proteins. The histidine-tagged proteins were then eluted using a linear gradient of up to 100% elution buffer E1 [50 mM tris(hydroxymethyl)aminomethane (Tris), 1 M NaCl, 1 M imidazole, 0.05% DDM, pH 7.0]. The eluted proteins were then further applied to a HiTrapQ ion-exchange column (GE Healthcare) at 4 °C in buffer III (50 mM Tris, 30 mM NaCl, 0.05% DDM, pH 7.5). Thereafter, the column was extensively washed with buffer III to remove nonspecifically bound proteins. The proteins were then eluted using a linear gradient of up to 100% elution buffer E2 (50 mM Tris, 2 M NaCl, 0.05% DDM, pH 7.5). The eluted proteins were then further purified on a Sephacryl S-400 HR gel filtration column (Amersham Biosciences) using buffer IV (50 mM Tris, 1 M NaCl, 0.05% DDM, pH 7.0). For FTIR measurements, the purified samples were reconstituted into PG liposomes (protein/phosphatidylglycerol = 1:30 molar ratio) by removing the detergent with SM2 Bio-Beads (Bio-Rad), as described elsewhere.[9] Notably, the absorption maxima of all of the labeled MR samples are identical to that of the unlabeled sample (Figure SI1B, Supporting Information), indicating no significant effect of the labeling on the isomeric composition of the proteins.

Time-Resolved Step-Scan FTIR Spectroscopy. TR-FTIR spectroscopy was employed to study structural changes

during the photocycles of the MR samples at ambient temperature. A 50 μL aliquot of a sample (5−7 mg/mL) was dried onto a BaF_2 window (ϕ = 25 mm, thickness = 2 mm), resulting in an absorbance of 0.9−1.1 for the amide I peak, and ∼8 microdrops of water containing 10% (v/v) glycerol were deposited near the sample to hydrate it. This method ensured moderate hydration conditions for suitable photoreaction and concomitantly reduced the infrared absorption of the O−H bending mode of water at approximately 1640 cm^{-1}, which overlaps with the amide I band of the protein. The sample was then closed by another window, separated by a silicone rubber ring, and sealed with Parafilm tape. The sample was mounted in a temperature-controlled transmission cell holder (TFC-M25-3, Harrick), and the temperature was maintained at 25 °C with circulating water in a thermostatted bath (Alpha RA8, Lauda). TR-FTIR spectra were recorded on a spectrometer (Vertex 80, Bruker Optics) equipped with a linearized MCT detector. The spectrometer was continuously purged with pure N_2 gas to reduce sharp peaks arising from background H_2O vapor. The photoreaction was triggered by a 532 nm laser pulse with a duration of 10 ns and a repetition rate of 10 Hz; the laser pulse was from the second harmonic generation of a Nd:YAG laser (LS-2134LS, LOTIS-TII). Using neutral density filters, light energy was regulated to be ∼1.6 mJ/pulse. The synchronization between the FTIR spectrometer and the laser apparatus was controlled by a digital delay generator (DG645, Stanford Research Systems). The resulting time and spectral resolutions were 12.5 μs and 4 cm^{-1}, respectively. An interferogram matrix $[\mathbf{I}(i, x)]$ was constructed after the data was collected at 999 sampling points (x) (mirror position). To construct the interferogram matrix, the light-induced transient signals were coadded nine times at 2000 time slices (i) (from −225 μs to 25 ms) at each fixed position (x) using the time-resolved step-scan mode. Each interferogram was converted to a single-beam spectrum via Fourier transformation between 850 and 1900 cm^{-1}. The 18 time slices recorded before the laser irradiation were used as a reference spectrum. To increase the quality of the spectra and to reduce the number of sampling points, infrared light with frequencies greater than 2000 cm^{-1} was removed using an IR filter (LP-5000, IR system). The spectra from ∼30 measurements were averaged for each set of sample conditions.

SVD and Global Fitting Analysis for TR-FTIR Data. To characterize the observed changes in TR-FTIR measurements, global exponential fitting was performed in combination with singular value decomposition (SVD) on all averaged spectral series obtained from each sample employing the methodology and personal MATLAB scripts developed by Dr. Víctor Lórenz-Fonfría.[10] The number of exponential components was estimated by global fitting of the most significant abstract time traces (**U** columns), i.e., those with comparably large associated singular values (**S** diagonal elements) and whose corresponding abstract spectrum (**V** columns) contained a signal more intense than the noise level. Then, the raw experimental data (not the SVD-reconstructed data) was globally fitted using the same number of exponential components, which provided the decay-associated spectra (DAS) (also known as the amplitude spectra):

$$\text{Data} = A\left(\sum_i \text{DAS}_i \exp(-k_i t) + \text{DAS}_3\right)$$

where i represents the number of resolved intermediates with the respective time constants k_i; DAS_3 is an offset, which indicates an unresolved intermediate with a decay time constant slower than could be resolved in the experiment; and A is a normalized factor for comparing the DAS of the isotope-labeled samples with those of unlabeled samples (the unlabeled sample with H_2O and D_2O hydration as a standard). Each value of A is shown in the captions of Figures 3, 4, and 5.

HPLC Analysis and Measurement of Resonance Raman Spectra. The retinal composition was determined by HPLC analysis, as described previously.[11−13] For light adaptation, the samples were irradiated for 5 min with yellow light through a 480 nm long-pass filter (Y48, Sigma Koki). Resonance Raman spectroscopy was performed using procedures, devices, and methods similar to those described previously.[14,15] Briefly, approximately 1 mL of a 50 μM MR solution was placed into a quartz spinning cell (diameter = 10 mm). A 0.5 M sodium sulfate solution added to buffer IV was used as an internal standard for Raman intensity measurements. The resonance Raman scattering was excited by the 514.5 nm line of an Ar^+-ion laser (BeamLok 2060, Spectra Physics). The laser power at the sample point was 1 mW. The Raman spectra were calibrated with cyclohexane and toluene. Sample integrity after exposure to the laser light was carefully confirmed by comparison of the visible absorption spectra obtained before and after the resonance Raman measurements.

RESULTS

Retinal Composition in PG-Reconstituted MR. In this study, TR-FTIR spectroscopy was performed on the light-adapted MR sample, which is inevitably formed by successive laser irradiation. We previously reported that dark-adapted MR consists of proteins that bind to all-*trans* (36.5%), 13-*cis* (56.4%), and 11-*cis* (7.6%) retinal in DDM micelles.[4] Upon illumination, all-*trans* retinal predominantly transformed into the 11-*cis* (30.1%) and 13-*cis* (47.7%) isomers, indicating the conversion from the all-*trans* to the 11-*cis* isomers. For the TR-FTIR study, we reconstituted MR samples into PG liposomes, where the composition of the retinal isomers has not been examined. Table 1 shows the retinal compositions of the MR sample reconstituted into PG liposomes in the dark and under illumination. As evident from the results in the table, in the dark, the main retinal configurations were all-*trans* (58.2%) and 13-*cis* (38.9%). Upon illumination with yellow light through a 480 nm long-pass filter for 5 min, the composition changed slightly: the percentages of the 11-*cis* (2.9% → 9.6%) and 13-*cis* (38.9% → 39.8%) retinal isomers increased, whereas the percentage of the all-*trans* isomer (58.2 → 49.3%) decreased. Thus, the all-*trans* isomer is a major component in PG-reconstituted MR. Notably, a light-dependent increase of the 11-*cis* isomer was commonly observed both in DDM micelles and in PG liposomes as the concentration of the all-*trans* isomer decreased, suggesting that similar structural changes probably occur upon light adaptation under both conditions.

Table 1. Retinal Configuration of MR Reconstituted into PG Liposomes in the Dark and under Illumination[a]

isomer	dark	light	dif.
all-*trans*	58.2 ± 1.2	49.3 ± 2.5	−8.9
13-*cis*	38.9 ± 1.2	39.8 ± 0.6	+0.9
11-*cis*	2.9 ± 0.6	9.6 ± 0.5	+6.7

[a]Three independent experiments were performed, and the results were averaged. The errors represents the standard deviations.

dx.doi.org/10.1021/jp308765t | J. Phys. Chem. B 2013, 117, 3449−3458

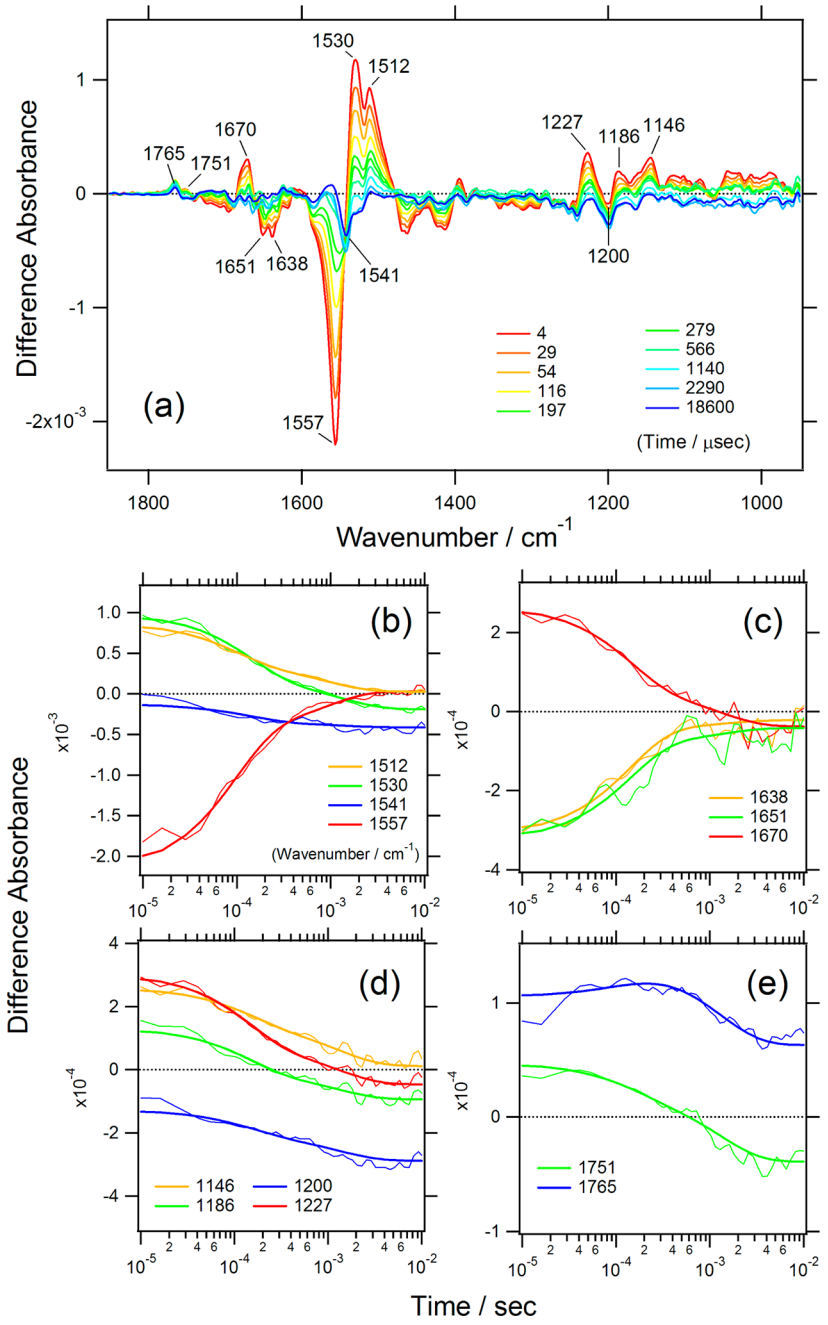

Figure 1. (a) Time-resolved FTIR difference spectra at the selected time slices. The spectra were logarithmically averaged to contain 20 data points per one log unit. The graphs in the lower panel show the time traces of the peaks at 1512, 1530, 1541, and 1557 cm^{-1} (b), 1638, 1651, and 1670 cm^{-1} (c), 1146, 1186, 1200, and 1227 cm^{-1} (d), and 1751 and 1765 cm^{-1} (e). Thick solid lines were obtained by global exponential fitting to the averaged data shown with thin solid lines.

Infrared Spectral Changes during the Photocycles of MR. In this study, we employed TR-FTIR spectroscopy with excitation by laser pulses to analyze structural changes during the photocycles of MR—structural changes in both the protein moiety and its chromophore, retinal (Figure 1). The spectra were analyzed by the global exponential fitting procedure in combination with SVD and were globally fitted with two exponentials (τ_1 = 95 ± 8 μs and τ_2 = 0.9 ± 0.2 ms) and a constant (Figure 1b–e). The value of this constant indicates the existence of a long-lived intermediate with a decay time longer than ~10 ms, which could not be determined in our experiments because of the limited observation time range (up to 25 ms). The high quality of the fit over the entire spectral and time range was confirmed, as shown in Figure 1b–e. These figures show the time traces of the bands of the amide II and/or the ethylenic stretches in the retinal region (b), in the amide I region (c), in the fingerprint region (d), and in the frequency region of carboxyl groups (e). The time constants τ of the components are summarized in Table 2, along with the previously identified values during the photocycles of MR in DDM micelles.[5] The differences in the values (after being assigned), on the one hand, could result from the fact that we studied MR reconstituted into PG liposomes and not into DDM micelles and, on the other hand, could result from the different fitting strategies used. Here the data has been globally fitted to the exponentials, whereas, in the case of the previous

dx.doi.org/10.1021/jp308765t | J. Phys. Chem. B 2013, 117, 3449–3458

Table 2. Lifetimes of MR in PG Liposomes Determined by FTIR Spectroscopy and Those of MR in DDM Micelles Determined by Laser Flash Photolysis[a]

τ_1 (μs)	τ_2 (ms)	τ of K from all-*trans*[b] (μs)	τ of M from all-*trans*[b] (ms)	τ of O-like from 13-*cis*[b] (ms)
95 ± 8	0.9 ± 0.2	93	12	5.1

[a]The τ_1 and τ_2 values indicate the lifetime of the exponential components identified by global fitting of the TR-FTIR data in Figure 1. [b]From ref 5.

study, a chosen region that exhibited the strongest change in the corresponding decay was fitted to obtain individual values.[5] The visible absorption band reflects the electronic state of the retinal chromophore, which is relatively easily classified into the specific ground or intermediate states in the photocycles of MR. However, vibrational modes of retinal, protein backbones, and amino acid residues in MR result in infrared absorption peaks, which are widely distributed in the observable spectral range and overlap with each other. Therefore, we performed global exponential fitting to extract DAS, which should be associated to specific intermediate states that can be detected by a visible-spectroscopy method, except in the cases of intermediates that are spectrally silent in the visible region.

Notably, although the PG-reconstituted sample also consists of all three isomers, as shown in Table 1, the 11-*cis* isomer is unlikely to be resolved in this study because of its fast photocycle and low concentration (9.6%) relative to those of the other isomers. For 13-*cis*, because a long excitation wavelength (532 nm) was employed, the activation of the all-*trans* isomer is likely greater than that of the 13-*cis* isomer.[5] To analyze the spectra more reliably and to support the assignment to the photocycles, three decay-associated spectra (DAS_1, DAS_2, and DAS_3) that correspond to the decay time constants of 95 μs, 0.9 ms, and >∼10 ms, respectively, were obtained using the global fitting procedure (Figure 2). Recent flash photolysis experiments of MR have revealed two red-shifted intermediates with decay time constants of 93 μs and 5.1 ms.[5] The former value is very similar to that of DAS_1. Therefore, the spectral transition of DAS_1 can be reasonably assigned to the decay process of the intermediate state with a decay time constant of 93 μs of MR(all-*trans*) in DDM micelles. However, the decay time constant of DAS_2 is substantially different from that of the intermediate state of MR(13-*cis*). DAS_2 may represent an intermediate that is spectrally silent in the visible region and that forms after the earlier intermediate characterized in DAS_1. However, MR has three isomers in the light-adapted state, and 40% of the 13-*cis* state remains in PG liposomes under illumination with light with a wavelength greater than 480 nm. Therefore, we cannot exclude the possibility that DAS_2 represents the intermediate state from the photocycle of MR(13-*cis*), whose difference in the time constant may be explained by different sample conditions (0.9 ms in PG liposomes or 5.1 ms in DDM micelles). Although, this study is focused on the spectral changes in the early photointermediate in the all-*trans* photocycle, two positive peaks at 1765 and 1751 cm^{-1} were observed in DAS_2; these peaks result from the protonation of carboxylate groups upon the formation of the DAS_2-associated intermediate. The decay time constant of DAS_2 under D_2O conditions was estimated to be 1.1 ± 0.3 ms, which is similar to that obtained under H_2O conditions (0.9 ms). Therefore, the protonation process should occur in the interior of the MR protein, not during uptake from

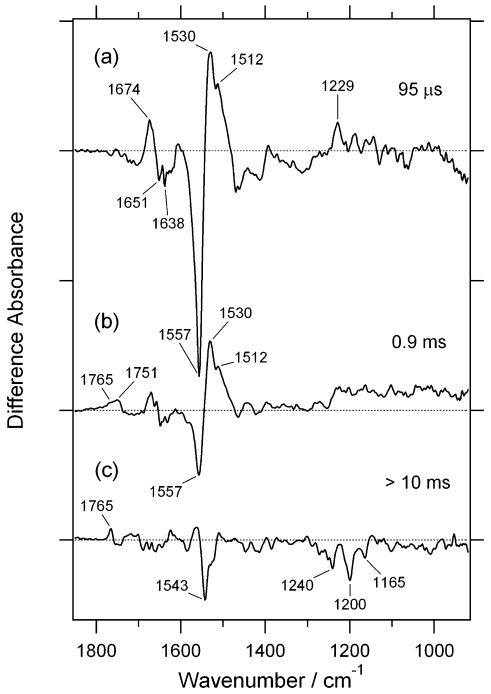

Figure 2. Decay-associated spectra (DAS) obtained by global exponential fitting analysis. DAS_1 (a), DAS_2 (b), and DAS_3 (c) show decay time constants of 95 μs, 0.9 ms, and >10 ms, respectively. One unit of the *y*-axis corresponds to 0.001 absorbance units.

the bulk phase. The possible donor for these carboxylates is the protonated Schiff base of the retinal chromophore. The deprotonation of the chromophore causes a drastic decrease in the intensity of infrared absorption and results in the appearance of negative bands in the fingerprint region, as shown in DAS_3. The configuration change also causes frequency shifts of the C−C stretching modes of the chromophore. The relatively small spectral change of DAS_2 in the fingerprint region suggests that both the protonation state and the configuration of the retinal chromophore do not change during this transition. Therefore, the proton donor should not be the protonated Schiff base and may be some amino acid residue(s) or water molecule(s) inside the protein.

DAS_3 is very similar to the difference infrared spectra recorded upon the formation of M intermediates of type-1 rhodopsins, such as bacteriorhodopsin and sensory rhodopsins.[16−18] The M intermediate is characterized by the deprotonated Schiff base that results from the transfer of a proton to a carboxylate counterion (Asp85 in BR and Asp75 in *p*SRII).[16,17] This counterion is also conserved in MR (Asp84); therefore, the positive peak at 1765 cm^{-1} probably corresponds to the protonation of Asp84 upon the formation of an M-like state. In previous flash photolysis experiments, an M intermediate was detected in the all-*trans* photocycle, with a decay time constant of 12 ms,[5] which is similar to our result (>∼10 ms). Furthermore, the assignment is supported by the fact that—typical for all-*trans* M intermediates—negative bands at 1240, 1200, and 1165 cm^{-1}, which are characteristic of the all-*trans* configuration, are assigned to the C—C stretching modes of all-*trans* retinal in the original state of MR, as described previously.[17] In addition, the negative band at 1543 cm^{-1} is assigned to the ethylenic C═C stretching vibration of the retinal chromophore because of a downshift of the peak in the samples reconstituted with isotopically labeled retinals

dx.doi.org/10.1021/jp308765t | J. Phys. Chem. B 2013, 117, 3449−3458

($^{13}C—C_{12}$, 1528 cm^{-1}; $^{13}C—C_{13}$, 1530 cm^{-1}; $C_{14}—D$, 1539 cm^{-1}; $C_{15}—D$, 1541 cm^{-1}). The frequency of the ethylenic mode correlates well with the λ_{max} in the visible absorption spectrum of the retinal chromophore. According to the literature,[19] 1543 cm^{-1} corresponds to ~510 nm, and this wavelength is close to that of the absorption maxima recorded for PG liposomes (504 nm; Figure SI1, Supporting Information). Thus, both DAS_1 and DAS_3 are successfully assigned to the all-*trans* photocycle, whereas DAS_2 is not assigned clearly to either the all-*trans* or the 13-*cis* photocycle. Therefore, two possibilities exist for the formation of the DAS_3 state: directly from the original light-adapted state after the DAS_1 transition or through the DAS_2 transition between the DAS_1 and DAS_3 transitions.

In this study, we focus on the early intermediate of MR(all-*trans*), which decays during the DAS_1 transition with a time constant of 95 μs because DAS_1 has a unique spectral shape, which particularly shows a distinct major positive band at 1229 cm^{-1} that has never been reported in previous FTIR experiments for type-1 rhodopsins.

Analysis and Interpretation of the Bands Observed upon the Formation of the Early Intermediate in the All-*trans* Photocycle. To investigate the origins of the bands in DAS_1 observed upon the formation of the early photointermediate in more detail (see Figures 3 and 4), we compared DAS obtained for MR samples with various isotopically labeled retinals (^{13}C-labeled proteins) with those obtained after an H/D exchange treatment (using D_2O that contained 10% $Gly(OD)_3$). Figure 3 focuses on the effects in the amide I [1674 (+), 1651 (−), and 1638 (−) cm^{-1}] and the amide II or the ethylenic C=C stretching modes of the retinal regions [1530 (+), 1512 (+), and 1557 (−) cm^{-1}]. The downshift of the bands in the amide I region to 1634 (+) and 1582 (−) cm^{-1} was observed in the MR sample with uniformly ^{13}C-labeled proteins (Figure 3a), supporting the assignment of the bands to the amide I modes of the MR protein. Although the positive band at 1674 cm^{-1} in the unlabeled protein can be easily connected with the 1634 cm^{-1} band in the uniformly ^{13}C-labeled protein, the shifts in the negative bands at 1651 and 1638 cm^{-1} may be perturbed presumably by the band overlap with the C=N stretching mode of the retinal Schiff base. This possibility was excluded using the sample with $C_{15}—D$-labeled retinal, as described later. In general, the spectrum of the amide I region may also be perturbed by the overlap with the O—H bending mode of water, as seen in the relatively large

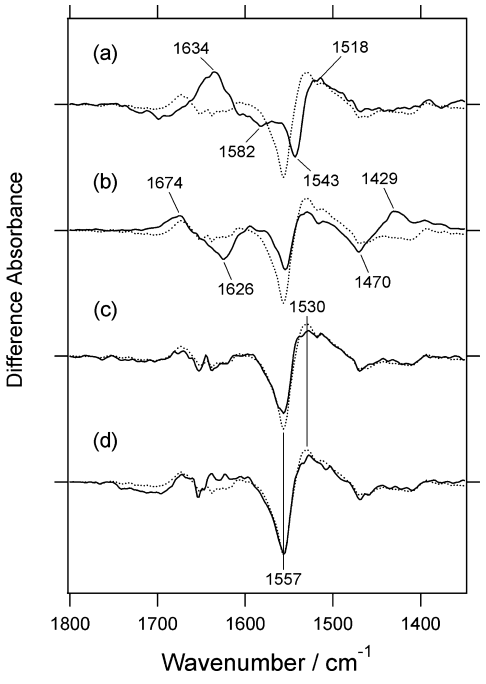

Figure 3. Amide I and II regions of DAS_1 of MR (a) with the ^{13}C-labeled protein moiety, (b) hydrated with D_2O containing 10% $Gly(OD)^3$, (c) reconstituted with retinal deuterated at the $C_{15}—H$ position, and (d) with the [4-^{13}C]Tyr-labeled protein moiety. The dotted line shows the spectrum of the unlabeled MR sample reproduced from Figure 2a. One unit of the *y*-axis corresponds to 0.003 absorbance units. The spectra were scaled to have intensities similar to those of the unlabeled MR sample by multiplying by 1.36 for the ^{13}C-labeled protein, by 1.95 for deuterated retinal at the C_{15} position, and by 2.6 for the [4-^{13}C]Tyr-labeled protein.

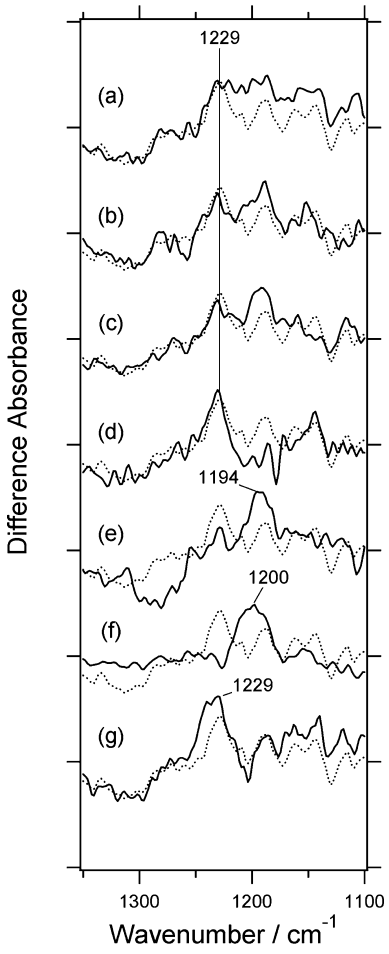

Figure 4. Fingerprint region of DAS_1 of MR reconstituted with retinal that was (a) ^{13}C-labeled at the C_{12} position, (b) ^{13}C-labeled at the C_{13} position, (c) deuterated at the $C_{14}—H$ position, and (d) deuterated at the $C_{15}—H$ position of retinal, or MR (e) with the ^{13}C-labeled protein moiety, (f) hydrated with D_2O containing 10% $Gly(OD)^3$, and (g) with the [4-^{13}C]Tyr-labeled protein moiety. The dotted lines show the spectrum of the unlabeled MR sample reproduced from Figure 2a. One unit of the *y*-axis corresponds to 0.0005 absorbance units. The spectra were scaled to have intensities similar to those of the unlabeled MR sample using a multiplication factor of 1.68 for ^{13}C-labeled retinal at the C_{12} position, 2.1 for ^{13}C-labeled retinal at the C_{13} position, 1.95 for deuterated retinal at the C_{14} position or the C_{15} position, 1.36 for the ^{13}C-labeled protein, and 2.60 for the [4-^{13}C]Tyr-labeled protein.

dx.doi.org/10.1021/jp308765t | J. Phys. Chem. B 2013, 117, 3449−3458

fluctuation of the time trace at 1651 cm^{-1} (Figure 1c). The influence could be omitted using D_2O to hydrate the sample. Amide I bands are expected to be only slightly affected by the H-to-D exchange because the bands mostly result from the C═O stretching vibrations. The amide I bands measured in D_2O are referred to as amide I′ bands. Figure 3b shows the TR-FTIR spectrum recorded under D_2O conditions. Two strong bands (1674 (+) and 1626 (−) cm^{-1}) were observed, which were assumed to result from the amide I′ modes. The former band appeared at the same frequency as the amide I band at 1674 cm^{-1} in H_2O. The frequency (1674 cm^{-1}) is typical for turn structures in proteins.[20,21] The latter band in D_2O is probably due to the amide I′ band that corresponds to the amide I band at 1638 cm^{-1} in H_2O, and both bands appear in the frequency region that is typical for β-sheet structures.[20] The frequency shifts (~12 cm^{-1}) upon the H/D exchange may result from uncoupling of vibrational coupling of the amide I mode of the protein backbone with O—H bending vibrations of water molecules that strongly interact with the peptide bonds. The relatively low frequency of the amide I′ band at 1626 cm^{-1} could be explained by a hydrated β-sheet structure, in accordance with a previous report.[22] In the case of C_{15}—D-labeled retinal (Figure 3c), all of the changes observed in the amide I region are quite similar to those of the unlabeled proteins (dotted line). This result suggests that C═N stretching of the Schiff base does not significantly change during the DAS_1 transition. Therefore, both the negative bands at 1651 and 1631 cm^{-1} are assigned to the amide I modes of the MR protein, as is the positive band at 1674 cm^{-1}.

According to previous experiments on retinal proteins, the bands at 1512 (+), 1530 (+), and 1557 (−) cm^{-1} could, in general, be assigned to the amide II mode or to the ethylenic stretching mode of the retinal chromophore in the ground state or in an intermediate state. However, the clear downshift caused by the ^{13}C labeling of the entire protein (Figure 3a) and the minor change induced by C_{15}–D labeling of the retinal chromophore (Figure 3c) support the assignment of the bands to amide II modes. Notably, although an amide II mode is mainly composed of the N–H bending vibration, it is altered by ^{13}C labeling because of coupling with the C–N stretch.[23] The shift of the amide II mode was observed in the absolute infrared absorption spectrum of the uniformly ^{13}C-labeled protein (Figure SI1A(e), Supporting Information), where the amide-II band shifted from 1545 to 1535 cm^{-1}. Thus, the intense band pair at 1530 (+)/1557 (−) cm^{-1} can be reasonably considered to originate mainly from amide II modes that were altered upon the formation of the early photointermediate. Furthermore, in the sample hydrated with D_2O, the bands assigned to the amide II modes are downshifted to 1429 (+)/1470 (−) cm^{-1} as a consequence of the H/D exchange of the peptide N–H groups (amide II′), suggesting that they exist in a hydrophilic part of the protein. The shoulder peak at 1512 (+) cm^{-1} is close to the typical frequency of a tyrosine-ring mode.[24] In the [4-^{13}C]Tyr-labeled sample (Figure 3d), we did not observe the distinct spectral downshift of the shoulder band to approximately 1477 cm^{-1} that had been reported in the literature.[25] Furthermore, the shoulder peak remains at the same frequency in the sample with C_{15}–D-labeled retinal (Figure 3c), suggesting that the peak does not arise from the ethylenic vibration of the retinal chromophore. From these results, in addition to the decreased susceptibility to the H/D exchange reaction in D_2O, the shoulder peak is assigned to the amide II mode in the hydrophobic part of the protein.

Figure 4 shows the effects induced by the isotopic labeling and the H/D exchange reaction with D_2O in the region between 1350 and 1100 cm^{-1}, where the C–C stretching vibrations of the retinal chromophore are mainly observed. A peak at approximately 1240–1220 cm^{-1} has been, in general, associated with the C_{12}–C_{13} stretch of the 11-*cis* retinal chromophore,[26] and would therefore indicate the photoisomerization from all-*trans* to 11-*cis*. In fact, HPLC experiments and static resonance Raman spectroscopy in the dark and under illumination clearly reveal that a positive peak appeared at 1223 cm^{-1} as a result of an increase in the concentration of the 11-*cis* configuration (Figure SI2, Supporting Information); i.e., a positive peak at approximately 1223 cm^{-1} could be a candidate for the C_{12}–C_{13} stretch of the retinal chromophore. We examined the possibility that the 1229 cm^{-1} band resulted from the C_{12}–C_{13} stretch of the chromophore. However, the isotopic labeling of the chromophore was found to produce a rather small effect on the 1229 cm^{-1} band in Figure 4a–d. In particular, the C_{12}–C_{13} stretch should exhibit a large upshift in the C_{14}–D-labeled sample, as seen in Figure 5c, where the negative peak at 1240 cm^{-1}

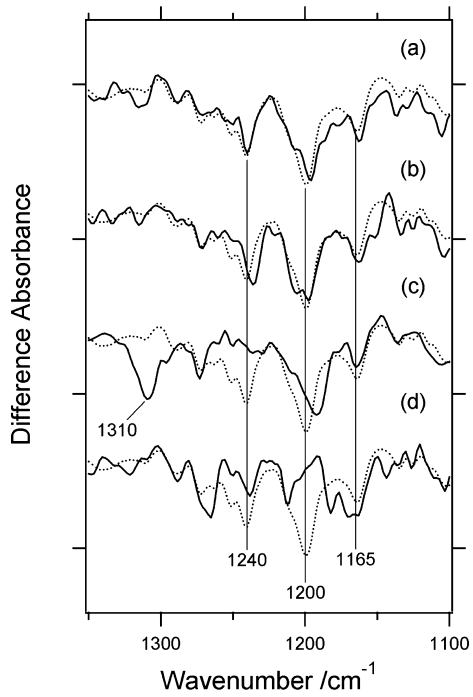

Figure 5. Fingerprint region of DAS_3 of MR reconstituted with retinal that was (a) ^{13}C-labeled at the C_{12} position, (b) ^{13}C-labeled at the C_{13} position, (c) deuterated at the C_{14}–H position, and (d) deuterated at the C_{15}–H position of retinal. The dotted lines show the spectrum of the unlabeled MR sample reproduced from Figure 2c. One unit of the *y*-axis corresponds to 0.0005 absorbance units. The spectra were scaled to have intensities similar to those of the unlabeled MR sample using a multiplication factor of 1.68 for ^{13}C-labeled retinal at the C_{12} position, 2.1 for ^{13}C-labeled retinal at the C_{13} position, and 1.95 for deuterated retinal at the C_{14} position or the C_{15} position.

exhibits a clear upshift to 1310 cm^{-1}. As a consequence, DAS_1 does not exclusively indicate that the photoisomerization from all-*trans* to 11-*cis* occurs in the photocycle of MR(all-*trans*). However, as previously mentioned, the intensities of the C–C stretching vibrations of the retinal chromophore in MR are relatively weak (Figures 1, 2, and 4), and therefore, the band of

dx.doi.org/10.1021/jp308765t | J. Phys. Chem. B 2013, 117, 3449–3458

the $C_{12}-C_{13}$ stretching vibration of the 11-*cis* isomer may not be detectable in this study. Future time-resolved resonance Raman spectroscopy studies may shed light onto the issue of the retinal conformation in the intermediates in the all-*trans* photocycle of MR.

Interestingly, a distinct effect was observed in the C−C stretching region of the TR-FTIR spectrum of the ^{13}C-labeled protein (Figure 4e), where the majority of the band at 1229 cm^{-1} was downshifted to 1194 cm^{-1}; this downshift suggests that this band is associated with some vibrations of the protein. In a previous study, the C−O stretching and C−O−H bending vibrations of the phenol ring in a tyrosine residue were shown to appear in the 1280−1165 cm^{-1} region.[24] This result suggests that the 1229 cm^{-1} band originates from the alteration of the hydrogen bond of the phenol O−H group of a tyrosine residue upon isomerization of the retinal chromophore. However, unexpectedly, the band did not exhibit a downshift in the [4-^{13}C]Tyr-labeled sample (Figure 4g), suggesting that the 1229 cm^{-1} band is assigned neither to the tyrosine C−O stretching and C−O−H bending modes nor to the $C_{12}-C_{13}$ stretching mode of 11-*cis* retinal. According to the literature, an amide III mode appears in the 1350−1200 cm^{-1} region with a considerably weaker intensity than those of the amide I and II modes.[27] The 1229 cm^{-1} band is likely due to the amide III mode because we have carefully excluded the most probable possibilities using the isotopically labeled samples. The band is located in the region typical of a β-sheet structure (1250−1220 cm^{-1}).[27] Therefore, it represents another piece of evidence that the β-sheet structure is perturbed upon the formation of the early photointermediate. The directions of the bands in the amide I and III regions are opposite, suggesting that the structural change cannot be simply interpreted as the destruction or construction of a β-sheet structure.

Indication of the Major Contribution of the All-*trans* Isomer to the Photoreaction of MR. Figure 5 shows DAS_3 in the C−C stretching region. The negative bands at 1240, 1200, and 1165 cm^{-1} are characteristic of the all-*trans* retinal chromophore and can be assigned to the $C_{12}-C_{13}$, $C_{14}-C_{15}$, and $C_{10}-C_{11}$ stretching modes, respectively.[28] These assignments have been confirmed via the isotopic labeling of the chromophore. The negative band at 1240 cm^{-1} was slightly downshifted in the spectrum of the ^{13}C-labeled sample at the C_{13} position (b) and largely upshifted to 1310 cm^{-1} in the spectrum of the C_{14}−D-labeled sample (c); these results are similar to those reported in the literature.[28] The assignment of the negative peak at 1200 cm^{-1} to the $C_{14}-C_{15}$ stretch of the all-*trans* isomer was supported by the downshift caused by the deuteration of retinal at the C_{15}−H position (d).

As previously mentioned, the M-like intermediate associated with DAS_3 is assumed to be directly formed from the DAS_1 transition or through the DAS_1 and DAS_2 transitions. The former case indicates that the DAS_1 and DAS_3 transitions are involved in the photocycle of the all-*trans* isomer of MR, and the latter case indicates that all of the observed transitions are involved.

DISCUSSION

Structure and Structural Changes of a β-Sheet in MR. Our results revealed that large spectral changes of the amide modes of a β-sheet occurred upon the formation of the early photointermediate, exhibiting a clear contrast to the small intensity of the retinal bands in DAS_1. In particular, the amide III mode has a considerably weak infrared activity and has never been observed in the light-induced difference spectrum of type-1 rhodopsin. The amide III band at 1229 cm^{-1} is in the frequency range that is typical of a β-sheet structure, suggesting that a large perturbation occurred in the β-sheet. However, the frequency change of the amide I bands from 1638 to 1674 cm^{-1} suggests the partial conversion of the β-sheet into a turn structure. The appearance of the positive peak at 1229 cm^{-1} of the amide III mode may complicate the interpretation. The conversion of the β-sheet may be explained by its structural properties in the early intermediate. The environment that surrounds the rest of the β-sheet is assumed to transform into an environment that exhibits a larger absorption coefficient of the amide III mode. Here we cannot discuss the structural change in more detail and only propose that some perturbation of the β-sheet structure in the hydrophilic part of the protein occurs upon the formation of the early photointermediate in MR(all-*trans*).

As is well-known, type-1 rhodopsins contain seven transmembrane α-helices; thus, the question arises as to where this observed β-sheet structure would be located. As shown in Figure 6, the crystal structure of BR[29] shows the β-sheet structure in the b−c loop at the extracellular surface, which is conserved among all type-1 rhodopsins whose crystal structures

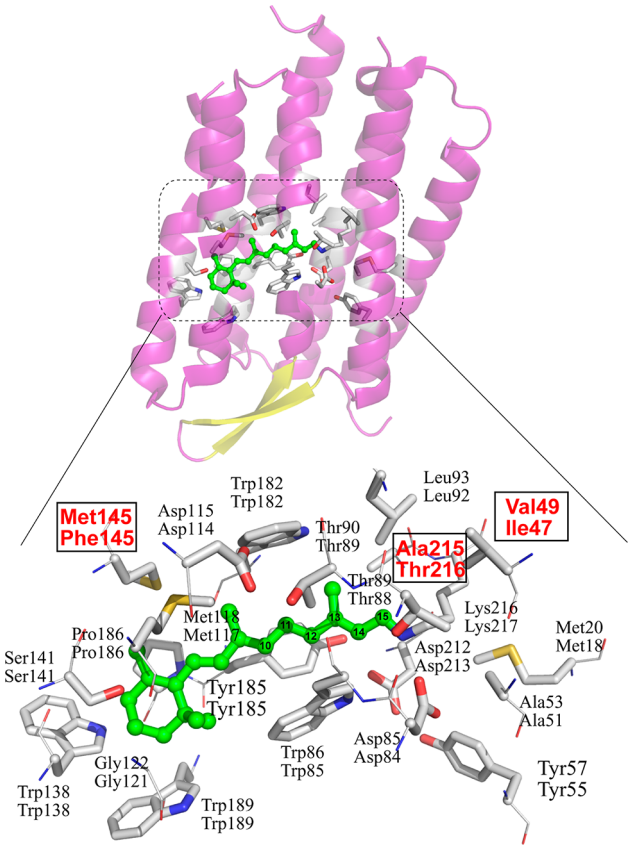

Figure 6. X-ray crystallographic structure of BR (1C3W)[29] and the magnified view of the retinal-binding pocket. BR contains seven transmembrane α-helices (colored purple) and one antiparallel β-sheet (colored yellow). The depicted amino acid residues contain the retinal-binding site located within 5 Å of the polyene chain or any methyl group of the retinal chromophore. The red-colored residues represent residues differing between BR and MR; the upper and lower labels are for BR and MR, respectively. The numbers on the polyene chain indicate the positions of the carbon atoms of the retinal.

dx.doi.org/10.1021/jp308765t | J. Phys. Chem. B 2013, 117, 3449−3458

have been solved, such as SRII, halorhodopsin (HR), and Anabaena sensory rhodopsin (ASR).[1,29−32] Although it is not possible to give the exact position of the β-sheet in MR owing to the lack of 3D structural information, it is likely located in the b−c loop, which must be in a hydrophilic environment. Notably, the β-sheet structure would therefore be considerably far from the retinal chromophore (∼20 Å), indicating that the relatively large structural changes in the β-sheet are caused by long-range interactions with the retinal chromophore. Furthermore, the structural changes in the β-sheet were not observed by low-temperature FTIR spectroscopy at 77 K,[4] supporting the distant location of the β-sheet and the large extent of the conformational change, both of which are, in general, inhibited at such a low temperature.

The question arises as to what causes this unique structural change. As previously mentioned, MR has been found to be an evolutionary intermediate between BR and SRII, with its amino acid sequence being distantly related to both BR and SRII (∼41% identity with BR and ∼35% identity with SRII).[33] Furthermore, MR contains the amino acid residues that are important for the proton-pumping function (Asp85, Asp96, Asp212, and Glu204 in BR), except for the equivalent of Glu194 in BR; it also contains the residues important for signal transduction (Tyr174 and Thr204 in SRII).[34] Thus, it is likely that, similar to other type-1 rhodopsins, MR contains seven transmembrane segments. Also, the lysine residue on helix G, and the aspartate residue (Asp84) on helix C, which is predicted to be necessary for the stabilization of the protonated Schiff base, are conserved in MR. However, the alteration of the β-sheet has not been observed in the early photoproducts of other type-1 rhodopsins (e.g., the K or L intermediates of BR and the K intermediate of *Np*SRII),[35−37] which makes the structural change unique to MR. Figure 6b shows the structure around the retinal chromophore based on the crystal structure of BR, with the numbering of the amino acid residues in either BR or MR. Interestingly, the amino acid residues of MR are very similar to those of BR, with only Val49, Met145, and Ala215 being replaced by Ile47, Phe145, and Thr216, respectively. Therefore, these residues and/or their long-range interactions with the β-sheet may be involved in the unique structural change. These residues may also be important for the biological function of MR because the all-*trans* isomer is thought to be involved in the function in all of the type-1 rhodopsins.[1,2] Further studies of the structural changes of MR with 11-*cis*, 13-*cis*, and all-*trans* isomers and of its structure−function relationship are needed to verify the importance of the observed changes.

CONCLUSIONS

We identified peculiar light-induced structural changes of the all-*trans* isomer of MR at the step of the early photointermediate with a decay time constant of 95 μs. These changes are attributed to a large perturbation in a β-sheet structure in the hydrophilic part of the protein. The other two intermediates with decay time constants of 0.9 and >10 ms were also identified via some characteristic vibrational bands, such as protonation signals of some carboxylate group(s) in the protein. Thus, MR shows unique structural changes that are not observed in other type-1 rhodopsins.

ASSOCIATED CONTENT

Supporting Information

Supporting results that consist of the absolute infrared and visible spectra of various MR samples used in this study (Figure SI1) and the data of HPLC analysis and the resonance Raman spectroscopy of MR in the dark- and light-adapted states (Figure SI2). This material is available free of charge via the Internet at http://pubs.acs.org.

AUTHOR INFORMATION

Corresponding Author

*E-mail: furutani@ims.ac.jp (Y.F.); z47867a@cc.nagoya-u.ac.jp (Y.S.).

Notes

The authors declare no competing financial interest.

ACKNOWLEDGMENTS

The present study was financially supported in part by a Grant-in-Aid for Scientific Research (KAKENHI) on a Priority Area (Area No. 477). This study was also supported by the Joint Studies Program (2009-2010) of the Institute for Molecular Science and by grants from the Japanese Ministry of Education, Culture, Sports, Science and Technology to Y.F. (22770159, 22018030, 21026016), T.O. (24590038), M.M. (23750015), A.W. (23590141), and Y.S. (22018010, 22121508, 23687019). We also thank Víctor A. Lórenz-Fonfría for the use of his data-analysis program. Finally, the authors would like to thank Enago (www.enago.jp) for the English language review.

REFERENCES

(1) Sudo, Y. *CRC Handbook of Organic Photochemistry and Photobiology*, 3rd ed.; CRC Press: Boca Raton, FL, 2012; pp 1173−1193.
(2) Spudich, J. L.; Yang, C. S.; Jung, K. H.; Spudich, E. N. *Annu. Rev. Cell Dev. Biol.* **2000**, *16*, 365−392.
(3) Shichida, Y.; Matsuyama, T. *Philos. Trans. R. Soc., B* **2009**, *364*, 2881−2895.
(4) Sudo, Y.; Ihara, K.; Kobayashi, S.; Suzuki, D.; Irieda, H.; Kikukawa, T.; Kandori, H.; Homma, M. *J. Biol. Chem.* **2011**, *286*, 5967−5976.
(5) Inoue, K.; Reissig, L.; Sakai, M.; Kobayashi, S.; Homma, M.; Fujii, M.; Kandori, H.; Sudo, Y. *J. Phys. Chem. B* **2012**, *115*, 4500−4508.
(6) Lugtenburg, J. *Pure Appl. Chem.* **1985**, *57*, 753−762.
(7) Sudo, Y.; Okuda, H.; Yamabi, M.; Fukuzaki, Y.; Mishima, M.; Kamo, N.; Kojima, C. *Biochemistry* **2005**, *44*, 6144−6152.
(8) Hayashi, K.; Sudo, Y.; Jee, J.; Mishima, M.; Hara, H.; Kamo, N.; Kojima, C. *Biochemistry* **2007**, *46*, 14380−14390.
(9) Sudo, Y.; Okada, A.; Suzuki, D.; Inoue, K.; Irieda, H.; Sakai, M.; Fujii, M.; Furutani, Y.; Kandori, H.; Homma, M. *Biochemistry* **2009**, *48*, 10136−10145.
(10) Lorenz-Fonfria, V. A.; Kandori, H. *J. Am. Chem. Soc.* **2009**, *131*, 5891−5901.
(11) Sudo, Y.; Yuasa, Y.; Shibata, J.; Suzuki, D.; Homma, M. *J. Biol. Chem.* **2011**, *286*, 11328−11336.
(12) Kitajima-Ihara, T.; Furutani, Y.; Suzuki, D.; Ihara, K.; Kandori, H.; Homma, M.; Sudo, Y. *J. Biol. Chem.* **2008**, *283*, 23533−23541.
(13) Suzuki, D.; Furutani, Y.; Inoue, K.; Kikukawa, T.; Sakai, M.; Fujii, M.; Kandori, H.; Homma, M.; Sudo, Y. *J. Mol. Biol.* **2009**, *392*, 48−62.
(14) Mizuno, M.; Kamikubo, H.; Kataoka, M.; Mizutani, Y. *J. Phys. Chem. B* **2011**, *115*, 9306−9310.
(15) Yamada, K.; Ishikawa, H.; Mizutani, Y. *J. Phys. Chem. B* **2012**, *116*, 1992−1998.
(16) Souvignier, G.; Gerwert, K. *Biophys. J.* **1992**, *63*, 1393−1405.

(17) Furutani, Y.; Iwamoto, M.; Shimono, K.; Kamo, N.; Kandori, H. *Biophys. J.* **2002**, *83*, 3482−3489.
(18) Furutani, Y.; Takahashi, H.; Sasaki, J.; Sudo, Y.; Spudich, J. L.; Kandori, H. *Biochemistry* **2008**, *47*, 2875−2883.
(19) Aton, B.; Doukas, A. G.; Callender, R. H.; Becher, B.; Ebrey, T. G. *Biochemistry* **1977**, *16*, 2995−2999.
(20) Barth, A.; Zscherp, C. *Q. Rev. Biophys.* **2002**, *35*, 369−430.
(21) Earnest, T. N.; Herzfeld, J.; Rothschild, K. J. *Biophys. J.* **1990**, *58*, 1539−1546.
(22) Kimura, T.; Maeda, A.; Nishiguchi, S.; Ishimori, K.; Morishima, I.; Konno, T.; Goto, Y.; Takahashi, S. *Proc. Natl. Acad. Sci. U.S.A.* **2008**, *105*, 13391−13396.
(23) Krimm, S.; Bandekar, J. *Adv. Protein Chem.* **1986**, *38*, 181−364.
(24) Takahashi, R.; Noguchi, T. *J. Phys. Chem. B* **2007**, *111*, 13833−13844.
(25) Takahashi, R.; Boussac, A.; Sugiura, M.; Noguchi, T. *Biochemistry* **2009**, *48*, 8994−9001.
(26) Palings, I.; Pardoen, J. A.; van den Berg, E.; Winkel, C.; Lugtenburg, J.; Mathies, R. A. *Biochemistry* **1987**, *26*, 2544−2556.
(27) Cai, S.; Singh, B. R. *Biophys. Chem.* **1999**, *80*, 7−20.
(28) Smith, S. O.; Braiman, M. S.; Myers, A. B.; Pardoen, J. A.; Courtin, J. M. L.; Winkel, C.; Lugtenburg, J.; Mathies, R. A. *J. Am. Chem. Soc.* **1987**, *109*, 3108−3125.
(29) Luecke, H.; Schobert, B.; Richter, H. T.; Cartailler, J. P.; Lanyi, J. K. *J. Mol. Biol.* **1999**, *291*, 899−911.
(30) Kolbe, M.; Besir, H.; Essen, L. O.; Oesterhelt, D. *Science* **2000**, *288*, 1390−1396.
(31) Luecke, H.; Schobert, B.; Lanyi, J. K.; Spudich, E. N.; Spudich, J. L. *Science* **2001**, *293*, 1499−1503.
(32) Vogeley, L.; Sineshchekov, O. A.; Trivedi, V. D.; Sasaki, J.; Spudich, J. L.; Luecke, H. *Science* **2004**, *306*, 1390−1393.
(33) Bolhuis, H.; Palm, P.; Wende, A.; Falb, M.; Rampp, M.; Rodriguez-Valera, F.; Pfeiffer, F.; Oesterhelt, D. *BMC Genomics* **2006**, *7*, 169.
(34) Sudo, Y.; Furutani, Y.; Kandori, H.; Spudich, J. L. *J. Biol. Chem.* **2006**, *281*, 34239−34245.
(35) Rothschild, K. J. *J. Bioenerg. Biomembr.* **1992**, *24*, 147−167.
(36) Hein, M.; Wegener, A. A.; Engelhard, M.; Siebert, F. *Biophys. J.* **2003**, *84*, 1208−1217.
(37) Lanyi, J. K. *Annu. Rev. Physiol.* **2004**, *66*, 665−688.